Unusual Kondo-hole effect and crystal-field frustration in Nd-doped CeRhIn$_5$

P. F. S. Rosa,[1,2] A. Oostra,[1] J. D. Thompson,[2] P. G. Pagliuso,[3] and Z. Fisk[1]

[1]*University of California, Irvine, California 92697-4574, USA*
[2]*Los Alamos National Laboratory, Los Alamos, New Mexico 87545, USA*
[3]*Instituto de Física "Gleb Wataghin," UNICAMP, Campinas-SP 13083-859, Brazil*

We investigate single crystals of Ce$_{1-x}$Nd$_x$RhIn$_5$ by means of x-ray-diffraction, microprobe, magnetic susceptibility, heat capacity, and electrical resistivity measurements. Our data reveal that the antiferromagnetic transition of CeRhIn$_5$, at $T_N^{Ce} = 3.8$ K, is linearly suppressed with x_{Nd}. We associate this effect with the presence of a "Kondo hole" created by Nd substitution. The extrapolation of T_N^{Ce} to zero temperature, however, occurs at $x_c \sim 0.3$, which is below the two-dimensional percolation limit found in Ce$_{1-x}$La$_x$RhIn$_5$. This result strongly suggests the presence of a crystal-field induced magnetic frustration. Near $x_{Nd} \sim 0.2$, the Ising antiferromagnetic order from Nd^{3+} ions is stabilized and T_N^{Nd} increases up to 11 K in NdRhIn$_5$. Our results shed light on the effects of magnetic doping in heavy-fermion antiferromagnets and stimulate the study of such systems under applied pressure.

I. INTRODUCTION

A remarkable variety of unexpected phenomena arises when magnetic impurities are introduced in a metal. One classical example is that of gold (Au) metal, which is, in its pure form, a good conductor displaying decreasing electrical resistance with decreasing temperature. A few parts per million of magnetic iron impurities in Au, however, cause the resistance to rise logarithmically at a material-specific Kondo impurity temperature T_K [1]. This so-called single-ion Kondo effect reflects the incoherent scattering of conduction electrons by the magnetic impurities introduced into the host [2]. In addition to introducing only a few parts per million of magnetic impurities, it is also possible to synthesize materials in which there is a periodic lattice of Kondo "impurities" coupled to the surrounding sea of itinerant electrons. At temperatures well above T_K, conduction electrons are scattered incoherently by the periodic array of Kondo impurities, but at much lower temperatures translational invariance of the impurities requires that a strongly renormalized Bloch state develop in which scattering is coherent [3].

A good example of these behaviors is found when La is replaced systematically by magnetic (Kondo) Ce ions in the nonmagnetic host LaCoIn$_5$ [4]. In the Kondo-lattice limit CeCoIn$_5$, the low-temperature resistivity is very small, and the compound hosts unconventional superconductivity in which the effective mass of electrons in the renormalized conduction bands is large [5]. If a small number of Ce atoms in CeCoIn$_5$ now is replaced by nonmagnetic La ions, a Kondo-impurity effect develops on the La ions. The absence of a Ce ion in the periodic Kondo lattice creates a "Kondo hole" such that La acts as a Kondo impurity and incoherently scatters electrons in the renormalized heavy conduction bands [6]. In the series Ce$_{1-x}$La$_x$CoIn$_5$, the system evolves at low temperatures as a function of x from a coherent Kondo lattice ($x = 0$) to a a collection of incoherently scattering Kondo impurities at $x \sim 0.4$. Interestingly, this cross-over coincides with the percolation limit of a two-dimensional (2D) square lattice on which the La/Ce ions sit. Not coincidentally, Kondo-hole behavior is observed in Ce$_{1-x}$La$_x$RhIn$_5$ where antiferromagnetic (AFM) order decreases linearly with La. In the limit $T_N \to 0$, the critical La concentration, $x_c \sim 40\%$, also reflects the percolation limit of the 2D square lattice [10].

Magnetic doping has not been extensively studied in CeCoIn$_5$ or other members within the Ce$_m M_n$In$_{3m+2n}$ ($M =$ transition metals Co, Rh, Ir, Pd, Pt; $n = 0,1,2$; $m = 1,2,3$) family of which it is a part. Recently, however, Nd doping in CeCoIn$_5$ at concentrations 5–10% has been shown to induce an unexpected magnetic state inside the zero-field superconducting phase [7]. Remarkably, the propagation vector and moment size of the incommensurate magnetic order in Ce$_{0.95}$Nd$_{0.05}$CoIn$_5$ are identical to those observed in the field-induced magnetically ordered phase in pure CeCoIn$_5$ (Q phase) [8,9]. These results indicate that the Nd ions are fundamentally changing the electronic system and not acting simply as a Kondo hole. To our knowledge, there is no report on the effects of magnetic doping in the AFM member CeRhIn$_5$. In the following we address the open questions (i) how will the Nd^{3+} ($J = 9/2$) spins interact with the AFM order of CeRhIn$_5$? and (ii) will there be a Kondo-hole effect when well-localized Nd^{3+} ions substitute the Ce^{3+} ($J = 5/2$) Kondo ions?

In this work, we report the first study of magnetic doping in CeRhIn$_5$ by means of x-ray-diffraction, microprobe, magnetization, heat capacity, and electrical resistivity measurements. Our data show that the AFM ordering temperature of CeRhIn$_5$ ($T_N^{Ce} = 3.8$ K) decreases linearly with Nd concentration, x_{Nd}, and extrapolates to zero at a critical Nd concentration of $x_c \sim 30\%$. Hence, in the dilute regime, Nd^{3+} ions behave as a free paramagnetic impurity, i.e., a moment-bearing Kondo hole in the Ce system. The fact that x_c is below the percolation limit indicates that there is an additional mechanism besides dilution of the Ce^{3+} moments causing the suppression of the magnetic order of the Ce sublattice. We argue that this mechanism is a crystal-field induced magnetic frustration, presumably due to the different spin configurations of CeRhIn$_5$ (easy c-axis magnetization but with ordered moments in-plane) and NdRhIn$_5$ (Ising spins along the c axis). In fact, around $x_{Nd} \sim 0.2$, the Ising AFM order of the Nd sublattice is stabilized and T_N^{Nd} increases up to 11 K in pure NdRhIn$_5$.

II. EXPERIMENTAL DETAILS

Single-crystalline samples of $Ce_{1-x}Nd_xRhIn_5$ ($x = 0, 0.05, 0.1, 0.15, 0.2, 0.3, 0.5, 0.7, 0.9, 1$) were grown by the In-flux technique. The crystallographic structure was verified by x-ray powder diffraction at room temperature. In addition, several samples were characterized by elemental analysis using a commercial energy dispersive spectroscopy (EDS) microprobe.

Magnetization measurements were performed using a commercial superconducting quantum interference device. The specific heat was measured using a commercial small mass calorimeter that employs a quasiadiabatic thermal relaxation technique. The in-plane electrical resistivity was obtained using a low-frequency ac resistance bridge and a four-contact configuration.

III. RESULTS

Figure 1(a) shows the actual Nd concentration obtained by EDS (x_{EDS}) as a function of the nominal Nd concentration $x_{nominal}$. The smooth and monotonic relationship between the x_{EDS} and $x_{nominal}$ indicates that Nd is being incorporated in the lattice. Further, the small error bars, Δx, point to a rather homogeneous distribution of Nd. In the extremes of the series, x_{EDS} has an error bar of $\Delta x \sim 0.02$. For Nd concentrations around 50%, a larger variation of $\Delta x = 0.05$ is observed, which is expected for concentrations in the middle of the series. We note, however, that Δx is the standard deviation accounting for different samples from the same batch and not for a single sample. On average, the variation within a single crystal (~ 0.01) is smaller than the standard deviation. These results indicate that Nd substitutes Ce homogeneously instead of producing an intergrown of $NdRhIn_5$. Herein, we will refer to the actual EDS concentration.

Figure 1(b) shows the lattice parameters obtained by powder x-ray diffraction as a function of Nd concentration. The x-ray powder patterns show that all members of the series crystallize in the tetragonal $HoCoGa_5$ structure and no
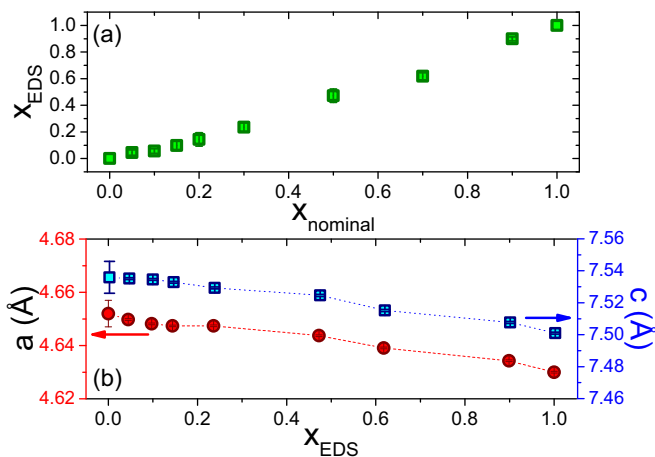
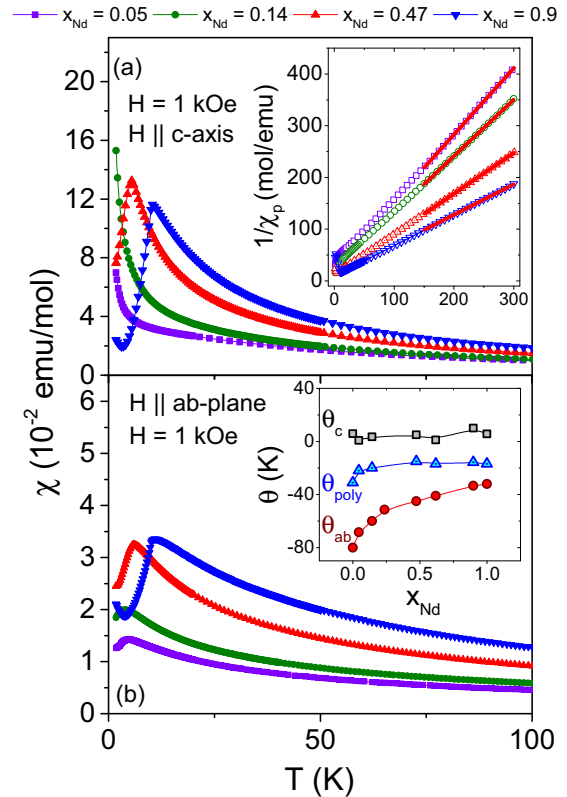FIG. 2. (a) Temperature dependence of the magnetic susceptibility, $\chi_c(T)$, of representative samples in the $Ce_{1-x}Nd_xRhIn_5$ series in a field of 1 kOe applied along the c axis. Inset: Inverse susceptibility of the polycrystalline average vs temperature. Solid lines are linear fits to the data. (b) Temperature dependence of the magnetic susceptibility, $\chi_{ab}(T)$, for the same samples in a field of 1 kOe applied along the ab plane. Inset: Curie-Weiss temperature, θ, for all compositions of $Ce_{1-x}Nd_xRhIn_5$.

additional peaks are observed. A smooth decrease is found in both lattice parameters a and c, in agreement with Vegard's law. This result implies that the volume of the unit cell is decreasing with Nd concentration, suggesting that Nd doping produces positive chemical pressure. Using the bulk modulus of $CeRhIn_5$, we estimate that a rigid shift of the lattice parameters from $CeRhIn_5$ to $Ce_{0.95}Nd_{0.05}RhIn_5$ corresponds to $\Delta P = 0.25$ GPa of applied pressure. From the phase diagram of $CeRhIn_5$ under pressure [11], this ΔP would correspond to an increase of T_N by 0.1 K. We will see below that the AFM order actually is suppressed in $Ce_{0.95}Nd_{0.05}RhIn_5$, indicating that chemical pressure is not the main tuning parameter determining T_N.

Figures 2(a) and 2(b) show the T dependence of the magnetic susceptibility, $\chi(T)$, for a field of 1 kOe applied along the c axis and ab plane, respectively. For low Nd concentrations ($x_{Nd} = 0.05, 0.14$), there is no evidence of T_N in the $\chi_c(T)$ data, i.e., when $H||c$-axis. This result is somewhat unexpected because AFM order is observed by a clear peak in heat capacity measurements of both $CeRhIn_5$ and $Ce_{1-x}Nd_xRhIn_5$. Instead of an expected peak in $\chi(T)$, we observe a low-T Curie tail, suggesting that the Nd ions are free paramagnetic impurities embedded in the Kondo lattice.

FIG. 1. (a) Actual concentration measured by EDS, x_{EDS}, as a function of nominal concentration, $x_{nominal}$ in the series $Ce_{1-x}Nd_xRhIn_5$. (b) Tetragonal lattice parameters as a function of x_{EDS} along the series $Ce_{1-x}Nd_xRhIn_5$.

When $H\|ab$-plane, however, $\chi_{ab}(T)$ displays a very similar behavior when compared to pure CeRhIn$_5$: there is a maximum in $\chi(T)$ followed by a kink at T_N^{Ce}. We attribute this difference to the fact that the spins in NdRhIn$_5$ point along the c axis and the magnetic susceptibility along this direction is much larger than the in-plane susceptibility. Thus, $\chi_{ab}(T)$ data reveal a linear decrease of $T_N^{Ce} = 3.8$ K with x_{Nd} up to $x_{Nd} = 0.14$. Between $x_{Nd} = 0.14$ and 0.23, the transition temperature starts to increase again, suggesting that the AFM order due to Nd ions starts to develop at T_N^{Nd}. Though not obvious in these data, $\chi_{ab}(T)$ reaches a maximum at $T_\chi^{max} > T_N^{Ce}$ in CeRhIn$_5$ and lightly Nd-doped samples. The temperature T_χ^{max} also decreases with x_{Nd}, from ~ 7.5 K in pure CeRhIn$_5$ to ~ 3.2 K at $x_{Nd} = 0.23$. Evidence for T_χ^{max}, however, is lost for $x_{Nd} > 0.23$ due to the dominant contribution from the Nd AFM order. We will return to this analysis when discussing the phase diagram of Fig. 5. Finally, for higher Nd concentrations, both $\chi_c(T)$ and $\chi_{ab}(T)$ show AFM behavior of a typical local moment system.

From fits of the polycrystalline average of the data [inset of Fig. 2(a)] to a Curie-Weiss law, we obtain effective magnetic moments of 2.5(1) μ_B, 2.7(1) μ_B, 3.2(1) μ_B, and 3.7(1) μ_B for $x_{Nd} = 0.05, 0.14, 0.47,$ and 0.9, respectively. These calculated values are in good agreement with the theoretical values of 2.59 μ_B, 2.69 μ_B, 3.05 μ_B, and 3.52 μ_B, respectively, considering the proper combination of the Ce^{3+} and Nd^{3+} effective moments. We also obtain the paramagnetic Curie-Weiss temperature, θ_{poly}, which averages out crystal electrical field (CEF) effects. The inset of Fig. 2(b) shows θ_{poly} as well as θ_c and θ_{ab}. In a molecular field approximation, θ_{poly} is proportional to the effective exchange interaction, J, between rare-earth ions. The fact that θ_{poly} is negative is in agreement with the AFM correlations found in the series. A reduction of θ_{poly} is observed going from CeRhIn$_5$ ($\theta_{poly} = -31$ K) to NdRhIn$_5$ ($\theta_{poly} = -17$ K), which suggests within a molecular field model that J also decreases along the series. As a consequence, this reduction in J would be expected to decrease the AFM ordering temperature. The experimental data, however, show the opposite behavior: T_N in NdRhIn$_5$ ($T_N^{Nd} = 11$ K) is almost three times larger than in CeRhIn$_5$ ($T_N^{Ce} = 3.8$ K). Moreover, in a Kondo lattice like CeRhIn$_5$, θ_{poly} also includes the AFM Kondo exchange that tends to reduce T_N relative to that expected solely from the indirect Ruderman-Kittel-Kasuya-Yosida (RKKY) interaction [12]. Because there is no Kondo effect in NdRhIn$_5$, the variation in θ_{poly} with x_{Nd} implies a suppression of the Kondo contribution and increased dominance of the RKKY interaction. This is reflected in the ratio T_N/θ_{poly}, which is 0.12 in CeRhIn$_5$ and 0.65 in NdRhIn$_5$. As illustrated in the inset of Fig. 2(b), θ_{poly} reaches a plateau between $x_{Nd} = 0.23$ and 0.47, suggesting that Kondo interactions are essentially quenched before $x_{Nd} = 0.47$. Consequently, one might expect T_N to increase initially as Nd replaces Ce and then to remain approximately constant for $x_{Nd} > 0.47$. As we will come to, this is not the case and T_N is a nonmonotonic function of Nd content. The above discussion indicates that there is another relevant mechanism determining the magnetic ordering in Ce$_{1-x}$Nd$_x$RhIn$_5$. From the nearly constant values of θ_c and pronounced change of θ_{ab}, the anisotropy of which is a consequence of CEF effects, it is reasonable to expect that CEF effects play an
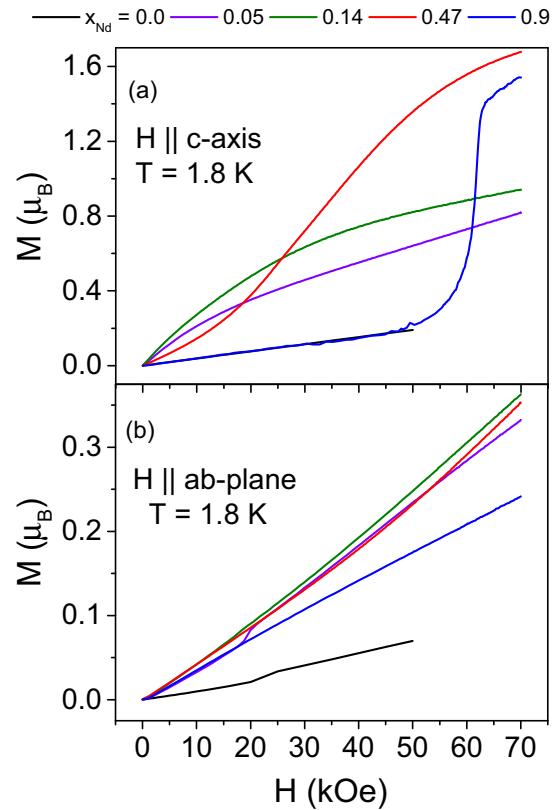

FIG. 3. (a) Field dependence of the magnetization at 1.8 K for fields along the c axis. Data for $x_{Nd} = 0$ coincide with that for $x_{Nd} = 0.9$ for $H \leqslant 50$ kOe. (b) Field dependence of the magnetization at 1.8 K for fields along the ab plane.

important role. In fact, from the high-temperature expansion of $\chi(T)$ we can readily observe that the main tetragonal CEF parameter, $B_2^0 \propto (\theta_{ab} - \theta_c)$, systematically decreases with Nd concentration.

Figures 3(a) and 3(b) show the H dependence of the magnetization, $M(H)$, at 1.8 K for fields applied along the c axis and ab plane, respectively. Although $M_c(H)$ for CeRhIn$_5$ displays a linear response with field, at low Nd concentrations ($x_{Nd} = 0.05, 0.14$) there is a nonlinear behavior that resembles a Brillouin function. This supports our interpretation of the origin of the low-T Curie tail in χ_c for low Nd content, namely, that Nd ions at low concentrations act as free paramagnetic entities. Because the Brillouin-like contribution to $M_c(H)$ is substantially larger than expected from just a simple free Nd moment, this behavior implies that Nd moments also are locally inducing free-moment-like character on neighboring Ce atoms. This is most pronounced for $H\|c$ due to the much higher susceptibility of Nd moments along this direction. At light Nd doping, then, Nd acts as a rather different type of Kondo hole compared to that induced by nonmagnetic La substitution for Ce. The Nd ions carry a net magnetic moment that is not quenched by the Kondo-impurity effect. At high x_{Nd}, $M_c(H)$ displays a field-induced transition to a spin-polarized state, as observed in NdRhIn$_5$. When the field is along the ab plane, pure CeRhIn$_5$ also displays a weak field-induced anomaly in $M_{ab}(H)$ ($H_c \sim 22$ kOe), which signals a change in ordering wave vector [13] and is suppressed with x_{Nd}.

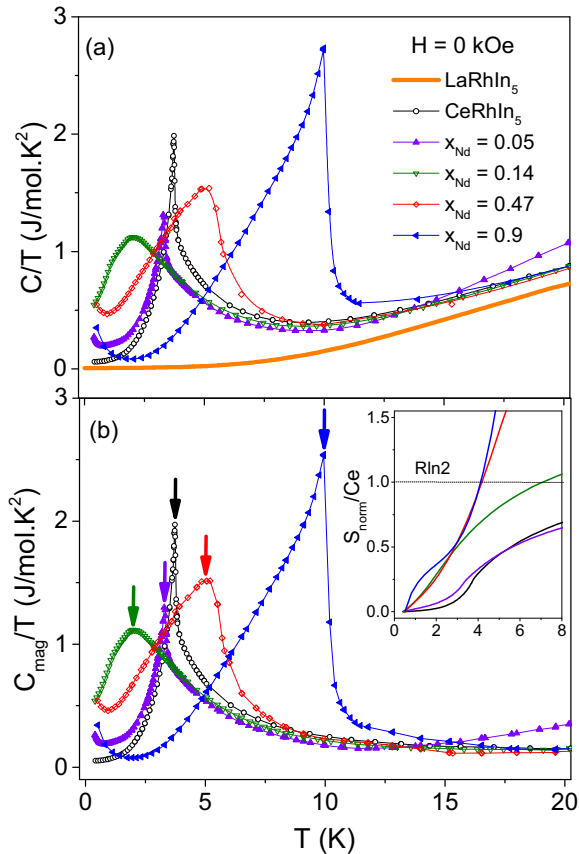FIG. 4. (a) Temperature dependence of the specific heat, C/T, of LaRhIn$_5$, CeRhIn$_5$ and representative samples of the series Ce$_{1-x}$Nd$_x$RhIn$_5$. (b) Magnetic contribution to the specific heat, C_{mag}/T, as a function of temperature. Inset: Entropy per Ce normalized by Rln2.

Figure 4(a) shows the temperature dependence of the heat capacity over temperature, C/T, for four representative Nd concentrations. LaRhIn$_5$, the nonmagnetic member, and pure CeRhIn$_5$ also are included. The sharp peak at $T_N = 3.8$ K displayed by CeRhIn$_5$ first decreases linearly with Nd concentrations up to $x_{\mathrm{Nd}} = 0.14$. At $x_{\mathrm{Nd}} = 0.14$, the transition at T_N starts to broaden and further increase in x_{Nd} reveals an enhancement of T_N, in agreement with $\chi(T)$ data.

Figure 4(b) shows the magnetic contribution to the heat capacity, C_{mag}/T, after subtracting LaRhIn$_5$ from the data. The transition temperature at which C_{mag}/T peaks is marked by the arrows. As the temperature is lowered further, an upturn is observed for all crystals with finite x_{Nd}, including NdRhIn$_5$, suggesting that the Nd ions are responsible for it. Reasonably, the upturn may be associated with the nuclear moment of Nd ions, and it can be fit well by a sum of both electronic ($\propto \gamma$) and nuclear ($\propto T^{-3}$) terms [14], consistent with the presence of a nuclear Schottky contribution.

The magnetic entropy as a function of temperature is obtained by integrating C_{mag}/T over T. The inset of Fig. 3(b) shows the T dependence of the magnetic entropy recovered per Ce ion. The entropy is normalized by Rln2, which is the entropy of the ground-state doublet. In pure CeRhIn$_5$ (black bottom curve), the magnetic entropy increases with T followed

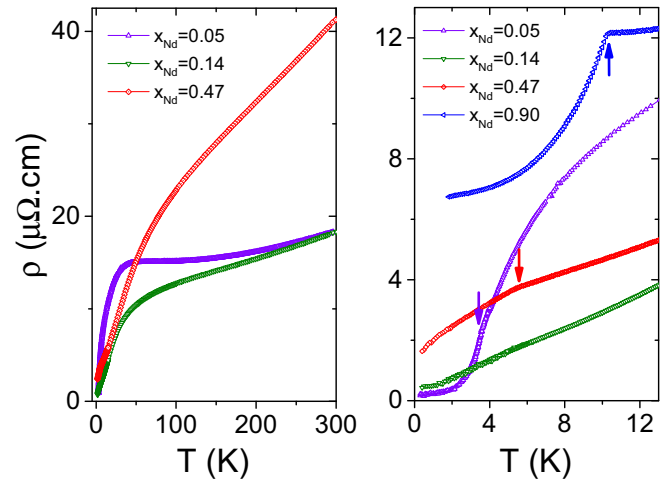FIG. 5. (a) In-plane electrical resistivity, $\rho_{ab}(T)$, of Ce$_{1-x}$Nd$_x$RhIn$_5$ as a function of temperature. (b) Low-temperature $\rho_{ab}(T)$ data. Arrows mark T_N.

by a kink at T_N. We observe an increase in the recovered entropy below T_N even when a very small amount of Nd is introduced (e.g., $x_{\mathrm{Nd}} = 0.05$). Increasing the concentration to $x_{\mathrm{Nd}} = 0.14$ yields a further entropy increase. This result indicates that the magnetic entropy does not scale with the Ce concentration, in turn suggesting that the extra magnetic entropy comes from the free paramagnetic Nd ions.

Finally, we discuss the temperature dependence of the in-plane electrical resistivity, $\rho_{ab}(T)$, of Ce$_{1-x}$Nd$_x$RhIn$_5$. Figure 5(a) shows $\rho_{ab}(T)$ for representative samples with $x_{\mathrm{Nd}} < 0.5$. At $x_{\mathrm{Nd}} = 0.05$, $\rho_{ab}(T)$ is very similar in magnitude and T dependence to that of pure CeRhIn$_5$. In particular, the broad peak at $\sim$40 K indicates the crossover from incoherent Kondo scattering at high temperatures to the heavy-electron state at low temperatures. As x_{Nd} is increased, $\rho_{ab}(T)$ decreases monotonically with temperature and the initial peak turns into a broad feature around 70 K when $x_{\mathrm{Nd}} = 0.47$. We note that the second CEF excited state of NdRhIn$_5$ is near 68 K, suggesting that the broad feature in $\rho_{ab}(T)$ is likely associated with CEF depopulation [15]. This evolution is consistent with an increase in the local character of the $4f$ system. Further, the low-temperature data shown in Fig. 5(b) display an increase in ρ_0. Typically disorder scattering would be expected to be a maximum near $x = 0.5$, but this is not the case. As shown in Ref. [15], the residual resistivity of pure NdRhIn$_5$ is much lower than that of our Ce$_{0.1}$Nd$_{0.9}$RhIn$_5$ crystal. This difference implies that spin-disorder scattering plays a significant role in determining ρ_0 in this series.

IV. DISCUSSION

In Fig. 6 we summarize our results in a $T - x$ phase diagram. We also include data of Ce$_{1-x}$La$_x$RhIn$_5$ from Ref. [10] for comparison. In the case of Ce$_{1-x}$Nd$_x$RhIn$_5$ two distinct regimes become clear. The first one, at low Nd concentrations, presents a linear decrease of T_N with x_{Nd}. Interestingly, a linear dependence of T_N also has been observed in Ce$_{1-x}$La$_x$RhIn$_5$, where La creates a Kondo hole in the system via dilution. We note that the creation of a Kondo hole
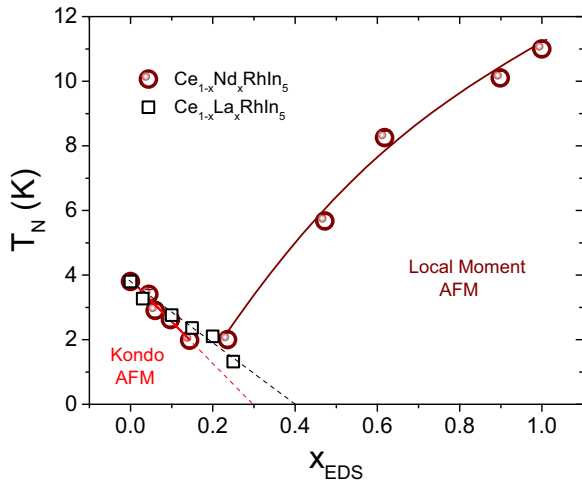
FIG. 6. $T - x$ phase diagram of the series $Ce_{1-x}La_xRhIn_5$ (from Ref. [10]) and $Ce_{1-x}Nd_xRhIn_5$ (this work).

by Nd^{3+} substitution in $CeRhIn_5$ is explained by the position of the Nd^{3+} $4f$ level, which is well below the Fermi level and generates well-localized moments. In the La-doping case, however, T_N extrapolates to $T = 0$ at a critical concentration of $x_c \sim 40\%$, which is the percolation limit of the 2D lattice. Here, Nd-doped $CeRhIn_5$ displays a smaller x_c of $\sim30\%$, indicating that there is an additional mechanism that frustrates Néel order in the Ce sublattice [10].

It has been shown—both theoretically and experimentally—that T_N in tetragonal structures is enhanced with respect to their cubic RIn_3 (R = rare-earth ions) counterparts whenever R has an Ising magnetic structure, i.e., spins polarized along the c axis [16–18]. This is due to the fact that the tetragonal CEF parameters in these structures favor a ground state with Ising symmetry, as supported by the fact that the c-axis susceptibility is larger than the ab-plane susceptibility in members whose R element has finite orbital momentum. Because $NdRhIn_5$ displays commensurate

Ising-like order below $T_N = 11$ K, it is reasonable to assume that Nd^{3+} ions will retain their Ising-like character when doped into the Ce sites [19]. $CeRhIn_5$, however, has an incommensurate magnetic structure with spins perpendicular to the c axis [20]. Hence, a crystal-field induced magnetic frustration of the in-plane order in $CeRhIn_5$ is induced by Nd^{3+} Ising spins. As a consequence, T_N^{Ce} of the Ce sublattice extrapolates to zero before the percolation limit and T_N^{Nd} of the Nd sublattice is stabilized.

V. CONCLUSIONS

In summary, we synthesize single crystals of $Ce_{1-x}Nd_xRhIn_5$ using the In-flux technique. X-ray-diffraction and microprobe measurements show a smooth evolution of lattice parameters and Nd concentration, respectively. Across the doping series, there is a complex interplay among Kondo-like impurity physics, magnetic exchange, and crystal-field effects as the Nd content changes. At low x_{Nd}, there is an unusual type of magnetic Kondo hole and T_N^{Ce} decreases linearly with x_{Nd}. The extrapolation of T_N^{Ce} to zero temperature occurs below the 2D percolation limit due to crystal-field induced magnetic frustration effects. Around $x_{Nd} \sim 0.2$, the Ising AFM order from Nd ions is stabilized and T_N^{Nd} increases up to 11 K in pure $NdRhIn_5$. Further investigation of the $Ce_{1-x}Nd_xRhIn_5$ series under pressure will be valuable to understand this interplay in the superconducting state.

[1] W. J. De Haas and G. J. Van Den Berg, Physica **3**, 440 (1936).

[2] J. Kondo, Prog. Theor. Phys. **32**, 37 (1964).

[3] G. R. Stewart, Rev. Mod. Phys. **56**, 755 (1984).

[4] S. Nakatsuji, S. Yeo, L. Balicas, Z. Fisk, P. Schlottmann, P. G. Pagliuso, N. O. Moreno, J. L. Sarrao, and J. D. Thompson, Phys. Rev. Lett. **89**, 106402 (2002).

[5] R. Settai, H. Shishido, S. Ikeda, Y. Murakawa, M. Nakashima, D. Aoki, Y. Haga, H. Harima, and Y. Onuk, J. Phys. Condens. Matter **13**, L627 (2001).

[6] E. D. Bauer, Yi-feng Yang, C. Capan, R. R. Urbano, C. F. Miclea, H. Sakai, F. Ronning, M. J. Graf, A. V. Balatsky, R. Movshovich, A. D. Bianchi, A. P. Reyes, P. L. Kuhns, J. D. Thompson, and Z. Fisk, Proc. Natl. Acad. Sci. USA **108**, 6857 (2011).

[7] R. Hu, Y. Lee, J. Hudis, V. F. Mitrovic, and C. Petrovic, Phys. Rev. B **77**, 165129 (2008).

[8] S. Raymond, S. M. Ramos, D. Aoki, G. Knebel, V. P. Mineev, and G. Lapertot, J. Phys. Soc. Jpn. **83**, 013707 (2014).

[9] M. Kenzelmann, S. Gerber, N. Egetenmeyer, J. L. Gavilano, Th. Strassle, A. D. Bianchi, E. Ressouche, R. Movshovich, E. D. Bauer, J. L. Sarrao, and J. D. Thompson, Phys. Rev. Lett. **104**, 127001 (2010).

[10] P. G. Pagliuso, N. O. Moreno, N. J. Curro, J. D. Thompson, M. F. Hundley, J. L. Sarrao, Z. Fisk, A. D. Christianson, A. H. Lacerda, B. E. Light, and A. L. Cornelius, Phys. Rev. B **66**, 054433 (2002).

[11] T. Park, F. Ronning, H. Q. Yuan, M. B. Salamon, R. Movshovich, J. L. Sarrao, and J. D. Thompson, Nature (London) **440**, 65 (2006).

[12] S. Doniach, Physica B **91**, 231 (1977).

[13] S. Raymond, E. Ressouche, G. Knebel, D. Aoki and J. Flouquet, J. Phys.: Condens. Matter **19**, 242204 (2007).

[14] A. C. Anderson, B. Holmstrom, M. Krusius, and G. R. Pickett, Phys. Rev. **183**, 546 (1969).

[15] N. V. Hieu, T. Takeuchi, H. Shishido, C. Tonohiro, T. Yamada, H. Nakashima, K. Sugiyama, R. Settai, T. D. Matsuda, Y. Haga,

M. Hagiwara, K. Kindo, S. Araki, and Y. Nozue, and Y. Onuki, J. Phys. Soc. Jpn. **76**, 064702 (2007).

[16] P. G. Pagliuso, J. D. Thompson, M. F. Hundley, and J. L. Sarrao, Phys. Rev. B **62**, 12266 (2000).

[17] P. G. Pagliuso, D. J. Garcia, E. Miranda, E. Granado, R. Lora Serrano, C. Giles, J. G. S. Duque, R. R. Urbano, C. Rettori, J. D. Thompson, M. F. Hundley, and J. L. Sarrao, J. Appl. Phys. **99**, 08P703 (2006).

[18] R. Lora-Serrano, C. Giles, E. Granado, D. J. Garcia, E. Miranda, O. Agüero, L. Mendonça Ferreira, J. G. S. Duque, and P. G. Pagliuso, Phys. Rev. B **74**, 214404 (2006).

[19] S. Chang, P. G. Pagliuso, W. Bao, J. S. Gardner, I. P. Swainson, J. L. Sarrao, and H. Nakotte, Phys. Rev. B **66**, 132417 (2002).

[20] W. Bao, P. G. Pagliuso, J. L. Sarrao, J. D. Thompson, Z. Fisk, J. W. Lynn, and R. W. Erwin, Phys. Rev. B **62**, R14621(R) (2000).